Evidence for Active Control of Rectus Extraocular Muscle Pulleys

Joseph L. Demer,[1,2] *Sei Yeul Oh,*[1,3] *and Vadims Poukens*[1]

Purpose. Connective tissue structures constrain paths of the rectus extraocular muscles (EOMs), acting as pulleys and serving as functional EOM origins. This study was conducted to investigate the relationship of orbital and global EOM layers to pulleys and kinematic implications of this anatomy.

Methods. High-resolution magnetic resonance imaging (MRI) was used to define the anterior paths of rectus EOMs, as influenced by gaze direction in living subjects. Pulley tissues were examined at cadaveric dissections and surgical exposures. Human and monkey orbits were step and serially sectioned for histologic staining to distinguish EOM fiber layers in relationship to pulleys.

Results. MRI consistently demonstrated gaze-related shifts in the anteroposterior locations of human EOM path inflections, as well as shifts in components of the pulleys themselves. Histologic studies of human and monkey orbits confirmed gross examinations and surgical exposures to indicate that the orbital layer of each rectus EOM inserts on its corresponding pulley, rather than on the globe. Only the global layer of the EOM inserts on the sclera. This dual insertion was visualized in vivo by MRI in human horizontal rectus EOMs.

Conclusions. The authors propose the active-pulley hypothesis: By dual insertions the global layer of each rectus EOM rotates the globe while the orbital layer inserts on its pulley to position it linearly and thus influence the EOM's rotational axis. Pulley locations may also be altered in convergence. This overall arrangement is parsimoniously suited to account for numerous aspects of ocular dynamics and kinematics, including Listing's law. (*Invest Ophthalmol Vis Sci.* 2000;41: 1280–1290)

Initial attempts to mathematically model binocular alignment showed the importance to extraocular muscle (EOM) action of EOM paths and the pivotal mechanical role of orbital connective tissues. The need for EOM path data motivated early radiographic studies in monkeys[1] and humans,[2] suggesting that paths of rectus EOMs are stabilized relative to the orbit. A decade ago, Miller[3] used relatively low-resolution MRI with three-dimensional (3-D) reconstruction to demonstrate stability of rectus EOM belly paths throughout the oculomotor range.[3] The further demonstration by MRI that EOM paths are little affected by large surgical transpositions of their tendons provided strong evidence for EOM path constraint by pulleys coupled to the orbit.[4,5]

Recent anatomic studies of whole orbits confirmed that each rectus EOM passes through a pulley consisting of an encircling ring or sleeve of collagen, located near the globe equator in Tenon's fascia.[6,7] The microscopic structure of pulleys is stereotypic.[6–9] Pulley collagen fibrils are dense and organized in an interdigitating configuration suited to high internal rigidity.[10] Pulleys are coupled to the orbital wall, adjacent EOMs, and equatorial Tenon's fascia by bands containing collagen, elastin, and smooth muscle (SM). Abundant elastic fibers in and around pulleys[6,7] provide reversible extensibility essential to these resilient tissues.[11] Suspensory bands of the pulleys contain SM[6,7] with rich autonomic innervation.[7]

Pulleys have important implications for EOM action because the functional origin of an EOM is at its pulley.[12] It is thus not surprising that coronal plane locations of rectus pulleys, inferred from EOM paths in living subjects, are not only stereotypic in primary gaze, but are also stable in secondary gaze positions.[13] Evidence of the mechanical importance of pulleys is the finding that their heterotopy in the coronal plane is associated with predictable patterns of incomitant strabismus.[14] Theoretical studies of ocular kinematics suggest that suitable anteroposterior location of pulleys could implement a linear oculomotor plant, one that appears commutative to the brain.[15] Lower resolution MRI of rectus paths after surgical transposition of EOM insertions suggests that the anteroposterior location of pulleys is consistent with the foregoing theoretical requirements,[5] a finding now confirmed by higher resolution MRI of normal rectus EOM path inflections in secondary gaze positions (Clark and Demer, unpublished data, 2000).

Recent advances in orbital imaging technique have improved earlier orbital MRI resolution by an order of magnitude. Surprisingly, technical limitations in existing orbital anatomic data now make them inadequate for comparison to the increas-

From the [1]Department of Ophthalmology, Jules Stein Eye Institute, and the [2]Department of Neurology, University of California, Los Angeles; and the [3]Department of Ophthalmology, Samsung Medical Center, Sungkyunkwan University School of Medicine, Seoul, Korea.

Presented in part at the Wenner–Gren International Symposium on Advances in Strabismus Research: Basic and Clinical Aspects, June 25, 1999, Stockholm, Sweden.

Supported by US Public Health Service, National Eye Institute Grant EY-08313 and Core Grant EY-00331. JLD received a Research to Prevent Blindness Lew R. Wasserman merit award and is the Larraine and David Gerber Professor of Ophthalmology.

Submitted for publication September 14, 1999; revised December 9, 1999; accepted December 20, 1999.

Commercial relationships policy: N.

Corresponding author: Joseph L. Demer, Jules Stein Eye Institute, 100 Stein Plaza, UCLA, Los Angeles, CA 90095-7002. jld@ucla.edu.

Investigative Ophthalmology & Visual Science, May 2000, Vol. 41, No. 6

ing quality of modern MRI of living EOMs. A major limitation has resulted from exenteration of orbital tissues before histologic processing. Release of connective tissue tension in a nonphysiologic manner by dissection of individual EOMs from unfixed orbits can distort anatomic relationships. An improved technique involves en bloc exenteration of the orbital soft tissues from their bony supports, followed by fixation.[6,7] This method maintains most orbital topology, but not necessarily normal distances. Even so, dissection of the anterior periorbita from the orbital rim damaged the pulley supports. These artifacts limited interpretation of prior anatomic studies of the orbital connective tissues.

It has long been recognized that rectus EOMs of mammals contain two distinct layers.[16–20] The global layer contains three types of singly innervated fibers (SIFs) and one type of multiply innervated fiber (MIF); the orbital layer contains one type of SIF and one type of MIF. Classic studies have demonstrated that although the global layer is continuous from the annulus of Zinn to the tendinous insertion on the globe, the orbital layer terminates posterior to the scleral insertion.[16,21] Because these studies were performed before appreciation of the existence of pulleys, it is unclear from the literature how the EOM orbital layer may relate to contemporary understanding of pulley anatomy and function.

Technical improvements have made it possible to reconstruct detailed orbital histology without removal from the supporting bones, thus maintaining normal spatial relationships. The present study was thus designed to exploit improvements in MRI in living subjects, as well as histology in cadavers, for study of the precise relationship between EOM layers and the corresponding pulleys. These data were examined in the context of surgical exposures of living tissues and were interpreted in the context of contemporary concepts of the contribution of pulleys to binocular kinematics.

METHODS

Magnetic Resonance Imaging

High-resolution MR images were collected from volunteers who gave written, informed consent to a protocol conforming to the Declaration of Helsinki and approved by the Human Subject Protection Committee at the University of California, Los Angeles. Imaging was performed using a 1.5-T scanner (Signa; General Electric, Milwaukee, WI). Crucial aspects of this technique, described in detail elsewhere, include use of a dual-phased surface coil array (Medical Advances, Milwaukee, WI) to improve signal-to-noise ratio and fixation targets to avoid motion artifacts.[22] Images of 2-mm thickness in a matrix of 256 × 256 were obtained over a field of view of 8 cm for a resolution in plane of 312 μm. Axial images were obtained, as well as quasicoronal images perpendicular to the long axis of the orbit.

Tissue Preparation

Five human orbits (aged 44–93 years) were exenterated en bloc at autopsy through an intracranial approach within 24 hours of death. These were fixed for at least five days in 10% neutral buffered formalin with the periorbita intact but separated from bony support. Three additional human orbits (aged 17 months to 57 years) were obtained from a tissue bank (IIAM, Scranton, PA), in heads fresh frozen shortly after death. The frozen heads were slowly thawed in 10% neutral buffered formalin. Three monkeys, a rhesus (*Macaca mulatta*), a fascicularis (*Macaca fascicularis*), and a cebus (*Cebus apella*), were killed in conformity with recommendations of the American Veterinary Medical Association and ARVO Statement for the Use of Animals in Ophthalmic and Vision Research and perfused with fixative through the aorta. The intact, fixed right orbits of the three humans and three monkeys were then removed in continuity with the eyelids and orbital bones, the latter being carefully thinned under magnification by using a high speed-drill. These fixed right orbits were then decalcified for 24 hours at room temperature in 0.003 M EDTA and 1.35 N HCl. The left orbit of the cebus monkey was exenterated after fixation, and longitudinal dissections were made to remove each rectus EOM in continuity with its adjacent pulley and underlying sclera.

At autopsy of an adult male human conducted within 8 hours of death, all EOMs were harvested in continuity with their contiguous connective tissues. After atraumatic enucleation of the globes using surgical technique and magnification, EOMs were isolated and excised, with orientation carefully maintained. Representative EOMs and their contiguous pulleys were pinned to cardboard at anatomic length and orientation before fixation in 10% neutral buffered formalin.

Formalin-fixed tissues were dehydrated in graded solutions of alcohol and chloroform, embedded in paraffin, and serially sectioned at 10-μm thickness, as previously described.[6,7] Whole orbits were serially sectioned in the coronal plane. Individual human EOMs, as well as EOMs in continuity with the sclera in the cebus monkey, were step sectioned longitudinally in the vicinity of pulleys at intervals of 200 μm, and transversely at intervals of 200 μm posterior to them. All sections were mounted on gelatin-coated glass slides.

Masson's trichrome stain was used to show muscle and collagen and van Gieson's stain to show elastin.[23] As previously described,[7] SM was confirmed using monoclonal mouse antibody to human SM α-actin (Dako, Copenhagen, Denmark) applied at 4°C overnight at dilutions of 1:100 to 1:500. The antigen–antibody reaction for human SM α-actin was visualized using the ABC kit with blue chromogen (Alkaline Phosphatase Kit 3; Vector, Burlingame, CA).[24]

Orbital dissections were performed in three fresh adult human cadavers to isolate the medial rectus (MR) pulley. Selected tissues were excised and processed histologically to confirm their composition. Findings at these dissections were correlated with findings at routine strabismus surgeries performed by an author (JLD) in which rectus EOMs were exposed and clinical photographs taken.

RESULTS

MRI was performed in right and left gaze in six adult volunteers in axial image planes aligned with the horizontal rectus EOMs to visualize the fine structure of the insertions. Each horizontal EOM was typically represented in five adjacent image planes. Favorable image planes, ones typically including the superior or inferior regions of the horizontal rectus EOMs rather than in the central portion, consistently demonstrated the presence of one or more dark bands running anteriorly and peripherally toward the orbital rim. The dark bands were typically better demonstrated in different image planes for the MR and lateral

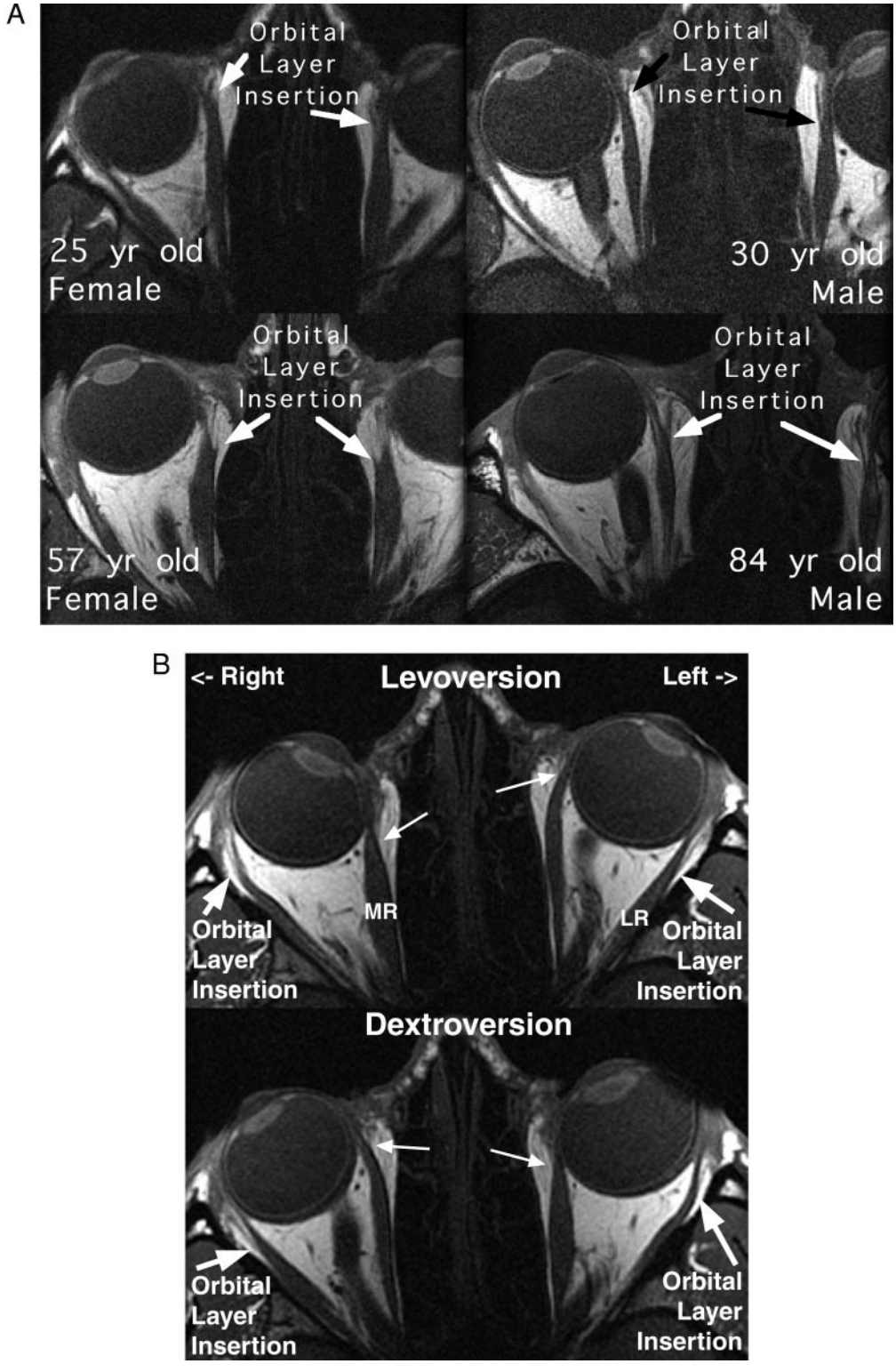

FIGURE 1. Axial MRI demonstrating dual insertions of horizontal rectus muscles in 2-mm-thick image planes at resolution of 312 μm. In each case, the *right* side of the subject is represented on the *left* side of the image. (**A**) Orbital layer insertion of MR muscles of four representative subjects of various ages fixating a target in dextroversion. Insertion of the orbital layer into the pulley (*arrows*) occurred roughly at the MR path inflection point and was generally farther posterior for the adducting left eye than for the abducting right eye. The dual nature of the MR insertion was more obvious in the older than in the younger subjects. A prosthetic intraocular lens is visible in the subject on the *lower right*. Images were intentionally decentered to favor the right orbit to improve resolution. (**B**) Orbital layer insertion of LR muscles on the corresponding pulleys of a representative subject in levoversion and dextroversion. *Thick arrows* denote insertion of the orbital layer on a *dark gray* band at the LR path inflection point produced by the LR pulley. Note the more posterior location of the LR orbital layer insertion in abduction than in adduction. The MR orbital layer insertion on the MR pulley is also visible (*thin arrows*).

rectus (LR) muscles. Histologic evidence indicates that this dark band represents the connective tissue suspension of the corresponding EOM pulley and that the orbital layer of the EOM inserts onto the connective tissue of the dark band.

The insertion of the MR orbital layer into its pulley is illustrated for four representative subjects of various ages in Figure 1A. In dextroversion, the MR path for the abducting right eye is inflected at roughly the point at which the dark band joins the EOM belly. This inflection, more obvious in image planes including the central part of the MR, corresponds to the MR pulley. The insertion of the dark band on the MR's orbital surface was more anterior in abduction than in adduction (Fig. 1A). More central image planes (for example, Fig. 1B) demonstrated a corresponding posterior shift in the MR inflection point with adduction. The dark band was more prominent in older subjects (Fig. 1A). These findings, supported by histo-

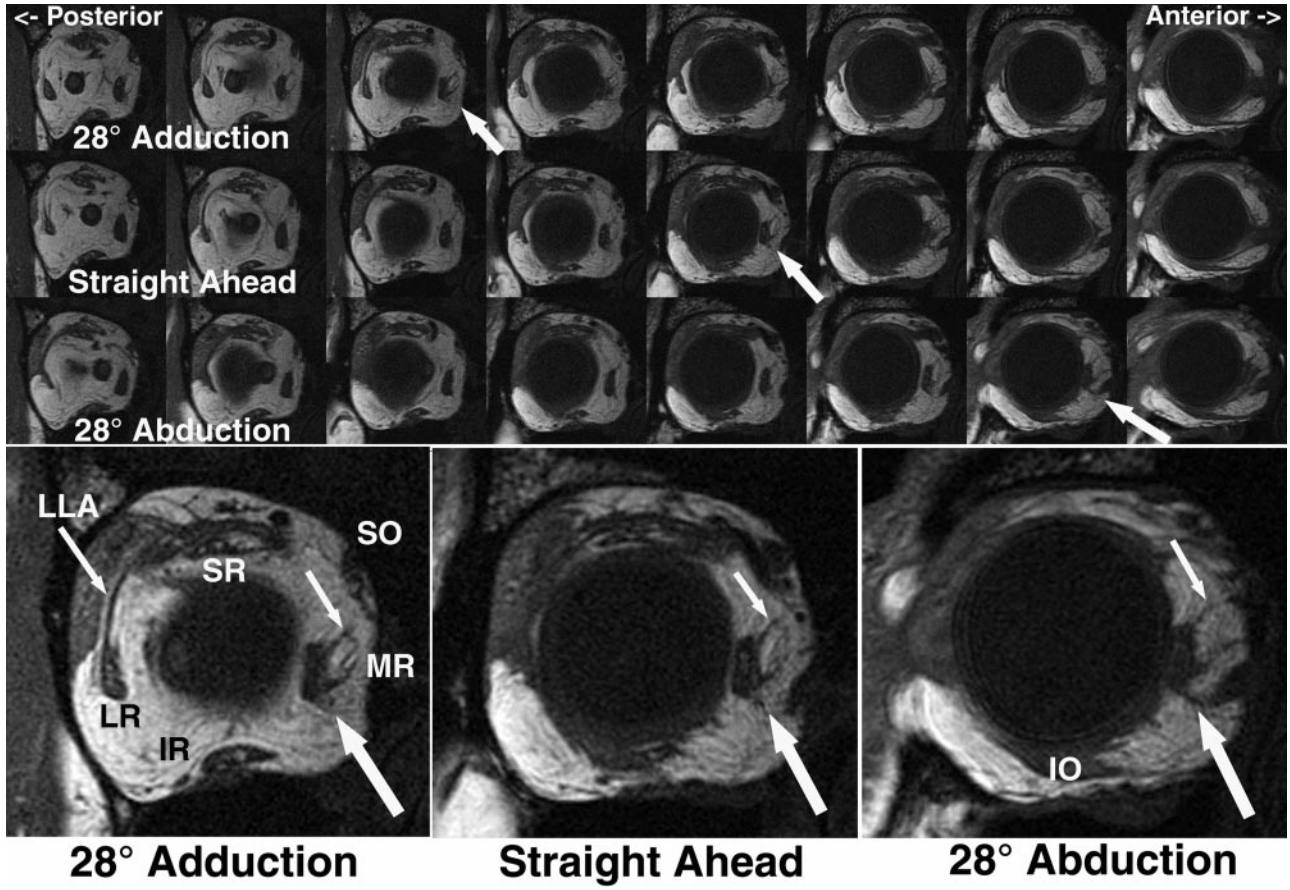

FIGURE 2. Sets of contiguous 2-mm-thick quasicoronal MRI images of a representative right orbit in 28° adduction, straight-ahead gaze, and abduction. Images are ordered from posterior at *left* to anterior at *right*, with identical head positioning for all gaze positions. The *thick white arrow* in each row demonstrates orbital layer insertion of the MR muscle on its pulley. The image planes including the insertion are enlarged in the *bottom* row for each gaze position. The insertion of the orbital layer is seen as three *dark* bands running radially toward the medial orbit. The orbital layer insertion was posterior in adduction and moved two image planes (4 mm) anteriorly in straight-ahead gaze and another two image planes (4 mm) anteriorly in abduction. IR, inferior rectus muscle; LLA, lateral levator aponeurosis; LR, lateral rectus muscle; MR, medial rectus muscle; SO, superior oblique muscle; SR, superior rectus muscle.

logic evidence below, indicate that the insertion of the MR orbital layer is on the MR pulley that in turn inflects the MR's path and that the pulley moves posteriorly from abduction to adduction.

A similar dark band was demonstrable for the LR muscle, originating at the path inflection produced by the LR pulley and extending anteriorly and laterally toward the orbital rim. Figure 1B demonstrates both prominent inflections produced by the horizontal rectus pulleys and the presence of dark bands at the inflections in dextro- and levoversion. The junction of the dark band with the LR moved posteriorly from abduction to adduction. Again, the junction of the dark band with the LR corresponds to the insertion of the LR orbital layer on its pulley.

Insertion of the orbital layer of horizontal rectus EOMs into the connective tissues of the peripheral orbit was also consistently appreciated in coronal plane imaging performed in eight subjects. The orbital layer insertion of the MR muscle could be visualized in nearly every orbit as one or more dark bands isodense with EOM extending radially toward the medial orbital wall (Fig. 2). The MR orbital layer insertion in Figure 2 typifies the most common pattern of three prominent bands. The anteroposterior extent of the orbital layer insertion was focal, so that it was imaged in only one or two adjacent 2-mm-thick coronal planes. As seen in Figure 2, large horizontal gaze shifts caused a corresponding shift in the anteroposterior location of the MR orbital layer insertion. In 28° adduction, the MR orbital layer insertion was relatively posterior at the level of the globe–optic nerve junction. In primary gaze, the MR orbital layer insertion moved two image planes (4 mm) and another two image planes (4 mm) anteriorly in 28° abduction for a total travel of approximately 8 mm.

Cadaveric and surgical dissections were begun sharply at the limbus and completed using only gentle blunt technique parallel to the rectus tendons. Each tendon was engaged at the insertion using a muscle hook, with which tension was applied to rotate the eye away from the EOM. The conjunctiva and adjacent connective tissues were retracted toward the orbital periphery. Cadaveric findings were consistent with intrasurgical findings using similar exposure. Figure 3 shows a surgical exposure of the MR, and illustrates multiple dense, white fibrous bands extending from the orbital surface of the MR muscle and inserting into the glistening white tissue on its nasal side. This adjacent connective tissue was confirmed in cadaveric material to form the pulley ring encircling the MR. During maximal abduction, the insertion of the MR orbital

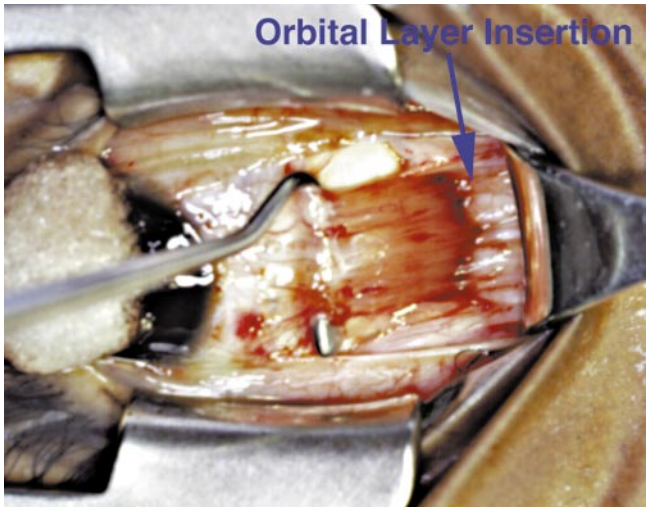

FIGURE 3. Surgical exposure of insertion of MR muscle on its pulley. A hook has been placed beneath the scleral insertion of the MR and traction applied to abduct the globe. The glistening *white* tissue at the aspect nasal of the MR (under tension from a retractor) forms the anterior part of the pulley and is joined to the orbital surface of the MR by fibrous bands located approximately 12 mm posterior to the scleral insertion of the MR with the eye maximally abducted. The cornea is partially covered by a pledget.

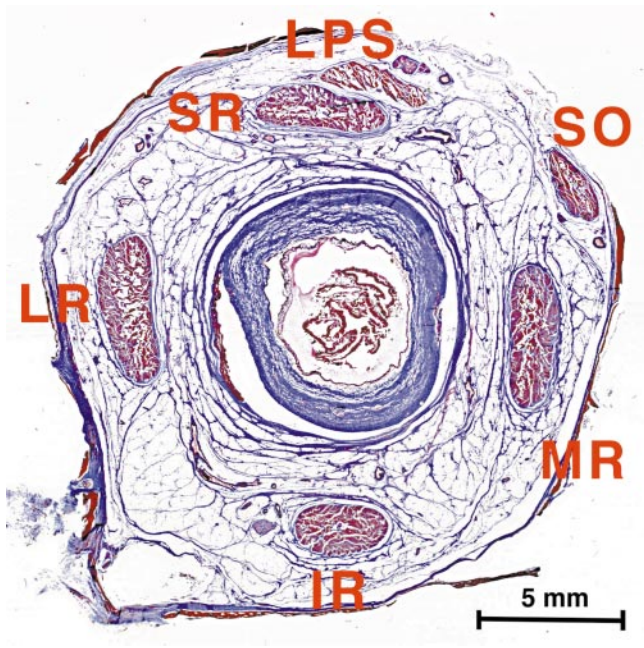

FIGURE 4. Low-power coronal photomicrograph of 17-month-old human right orbit stained with Masson's trichrome to distinguish orbital (more *purple* on surface) and global muscle (more *red* in EOM core and on global surface) fiber layers in the mid and posterior orbit. LPS does not have an orbital layer. Abbreviations as in Figure 2.

layer into its pulley was approximately 12 mm posterior to the insertion of the MR global layer on the sclera. This distance depends on horizontal eye position. Findings were similar for the other rectus EOMs.

Histochemistry and Immunohistochemistry

In low-power micrographs of the mid to posterior orbit where the orbital layer was present, Masson's trichrome stain clearly distinguished the global from the orbital layers of each rectus EOM on the basis of larger and redder fibers in the former, and the smaller, more purple fibers in the latter (Fig. 4). The distinction was clearer at higher power (Fig. 5). The orbital layer, where present, was always on the orbital surface of any EOM but typically encompassed most of the periphery of the EOM in a C-shape to include some of the global surface as well.[16] All fibers of the levator palpebrae superioris (LPS) resembled rectus global layer fibers. In the LPS an orbital layer was entirely absent. Serial sections were examined to locate the rectus pulleys, consisting of rings of dense collagen encircling the rectus EOMs. In every rectus EOM examined in humans and monkeys, fibers of the orbital layer inserted by short tendons in their respective pulleys and did not continue anteriorly to them. Thus, only the global layer of each EOM was continuous with the long insertional tendon on the globe. The orbital layer insertion of the LR on its pulley through short collagenous tendons is illustrated in Figure 5.

Van Gieson's elastin stain demonstrated dense elastin in the insertions of rectus orbital layers on their pulleys. Figures 6A and 6B are adjacent coronal sections at lower power demonstrating collagen (blue in Fig. 6A) and elastin (black in Fig. 6B) in a human MR pulley ring, at the point of orbital layer insertion. Higher power views of the lower right part of the image (black rectangle) demonstrate a bundle of orbital layer fibers completely surrounded by pulley collagen (Fig. 6C) stiffened by fine, black elastin fibers inserting directly on the muscle bundle itself (Fig. 6D).

In all orbits studied there was a prominent crescent of SM near the globe equator extending from the nasal border of the superior rectus (SR) pulley nasal to the MR pulley and terminating on the nasal border of the inferior rectus (IR) pulley. For consistency with Müller[25] (cited by Page[26]) this prominent deposit of SM will be referred to as the peribulbar muscle.

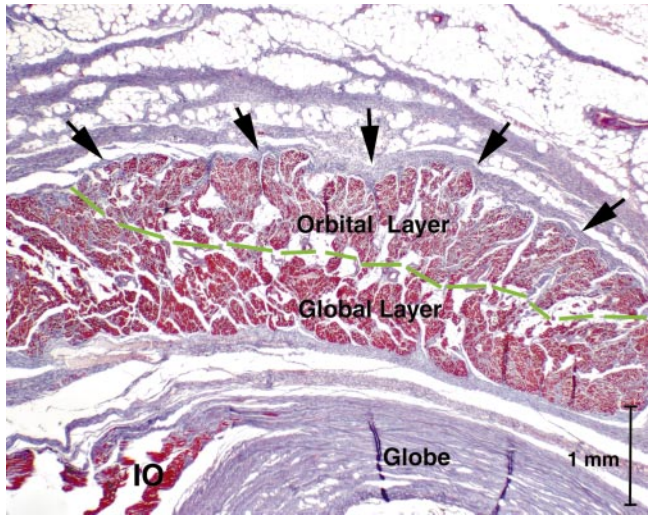

FIGURE 5. Higher power coronal photomicrograph of the LR of a 17-month-old human stained with Masson's trichrome demonstrating insertion of the orbital layer on fine, collagenous tendons (*arrowheads*) contiguous with the dense collagen (*blue*) of the LR pulley. Global layer fibers are brighter *red* than orbital layer fibers and are demarcated by the *broken green line*. IO, inferior oblique muscle.

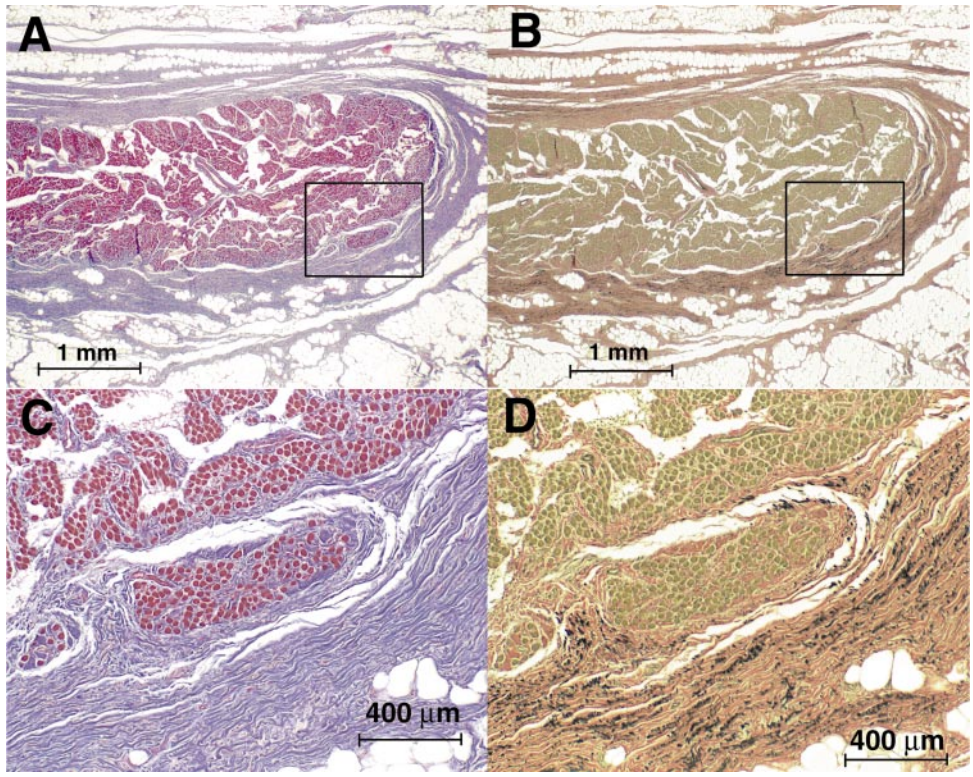

FIGURE 6. Adjacent 10-μm coronal sections of 17-month-old human MR stained with Masson's trichrome (**A**, **C**) and van Gieson's elastin stain (**B**, **D**) demonstrating insertion of the orbital layer on the encircling ring of the MR pulley. Fine rectangles at the *lower right* of (**A**) and (**C**) are magnified in (**B**) and (**D**) to demonstrate an orbital layer muscle fiber bundle completely encircled by dense collagen (*blue*) and penetrated by elastin fibrils (*black*) of the pulley.

The insertion of rectus orbital layer fibers on their respective pulleys was also confirmed by longitudinal sectioning of rectus EOMs in the cebus monkey orbit and in one human orbit. This is shown for a human LR in Fig. 7. The lower power view in Fig. 7A confirms that the orbital layer does not extend anteriorly to the LR pulley. The higher power view of the same region shown in Fig. 7B confirms that the orbital layer insertion is through particularly dense, short collagenous tendons that appear as focally dark blue terminations of orbital layer fibers.

DISCUSSION

Fundamental Anatomic Insight

Based on the number of abducens motor neurons, the average number of muscle fibers innervated by each neuron, and the average tension produced by each fiber, Goldberg et al.[27,28] estimated that the LR muscle should deliver approximately twice the force actually measured at its tendinous insertion on the globe during tetanic stimulation. The present study may partly explain the enigmatic question of what happened to the other half of the EOM force.[27] The MRI, gross anatomic, and histologic observations here support functional specialization of the two laminae of rectus EOMs. The global layer inserts on the sclera as classically recognized, but the orbital layer, consistent with its classic termination before the scleral insertion,[16,21,29] inserts instead on the corresponding pulley. We demonstrate elsewhere that the two EOM laminae contain roughly equal numbers of fibers.[30] The orbital layers are ideally placed to control the anteroposterior positions of the pulleys, moving them posteriorly during contraction as seen on axial MRI from the positions of the EOM path inflections (Fig. 1).

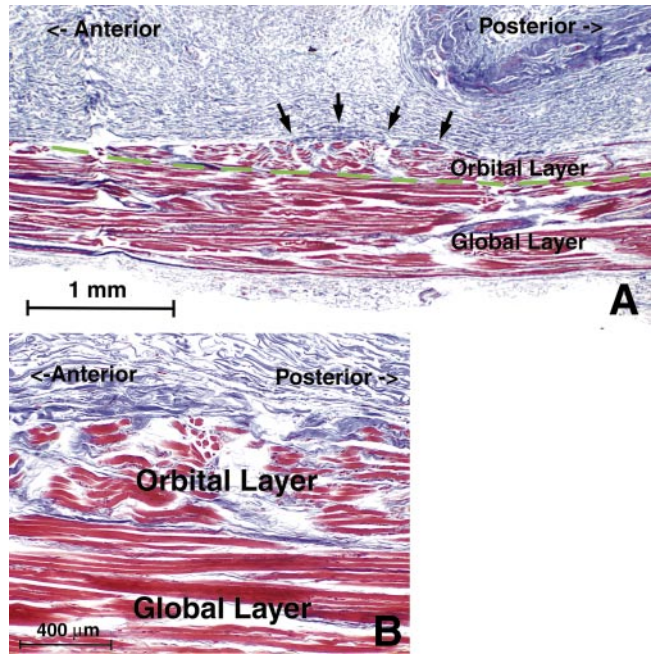

FIGURE 7. Longitudinal section of LR of a 57-year-old human stained with Masson's trichrome demonstrating insertion of the orbital layer into collagen of the pulley. (**A**) Low power. *Arrows* denote insertion of orbital layer fibers into *blue* pulley collagen. Junction between the *purple* orbital and *red* global layers delineated by a *green dotted line*. (**B**) Higher power. Note extensive interdigitation of pulley collagen with terminating orbital layer fibers.

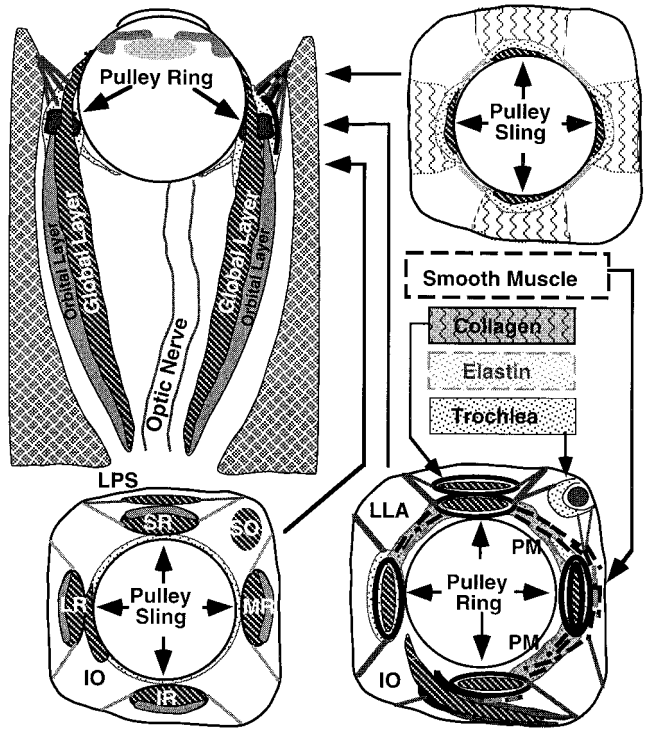

FIGURE 8. Structure of orbital connective tissues and their relationship to the fiber layers of the rectus muscles. Coronal views represented at levels indicated by *arrows* in horizontal section. PM, peribulbar smooth muscle. Remaining abbreviations as in Figure 2.

Corresponding anteroposterior motion of connective tissue components of the MR pulley with horizontal gaze are also demonstrable by axial (Fig. 1) and coronal (Fig. 2) MRI. The orbital layer of a rectus EOM probably exerts force on the sclera only indirectly, through changes in the path length of the global layer as determined by the location of the pulley. Contraction of the global layer of a rectus EOM mainly exerts force on the globe through the classic insertion and secondarily tends to stretch the fibromuscular pulley suspensions[6,7] that deflect the rectus EOM path away from a shorter straight-line path. Notwithstanding this indirect effect, it seems likely that most of the force of the global layer acts to rotate the globe, and most of the force of the orbital layer acts to position the corresponding pulley linearly. This emerging concept of the anatomy of the EOMs is diagrammed in Figure 8, and we term it the active-pulley hypothesis.

Implications for Ocular Kinematics

The pulleys are constituted to regulate ocular kinematics, the rotational properties of the eye. Rotations of any 3-D object are not mathematically commutative; that is, final eye orientation depends on the order of rotations.[31] Angular velocity of a 3-D object is not equal to the rate of change of its orientation but rather is a complex function related to both the time derivative and to instantaneous eye orientation.[32,33] Each combination of horizontal and vertical eye positions could, for an arbitrary 3-D object, be associated with infinitely many torsional positions.[34] The eye is fortunately constrained in its torsional freedom (with the head upright and immobile) by a relationship known as Donders' law, stating that there is only one torsional eye position for each combination of horizontal and vertical eye positions.[32] Listing's law, a specific case of the more general Donders' law, states that any physiologic eye orientation can be reached from any other by rotation around a single axis, and that all such possible axes lie in a single plane, Listing's plane. Listing's law is satisfied if for any eye movement the axis of ocular rotation shifts by exactly one half of the shift in ocular orientation.[33] This is the so-called Listing's half-angle rule.

Before pulleys were known, Listing's law was presumed to be implemented entirely by complex neural commands to the EOMs. However, experiments have not identified a neural substrate for Listing's law. In the superior colliculus, saccades are encoded as the two-dimensional (horizontal and vertical) rate of change of eye orientation, implying that any computation of the third dimension, torsion, is accomplished downstream.[15,35] Even in the oculomotor nucleus and rostral interstitial nucleus of the medial longitudinal fasciculus, saccadic burst commands are better correlated with rate of change of 3-D eye position than with angular eye velocity.[35,36] Nevertheless, Listing's law is presumed to have a neural basis[35] because it is systematically violated by the vestibulo-ocular reflex (VOR)[37] and during sleep.[38] The VOR is a phylogenetically ancient reflex that stabilizes images of fixed objects on the retina during head motion. An ideal VOR would have an axis of ocular rotation exactly matching that of the head, rather than shifting by half the change in eye orientation. Empirically, the axis of the VOR shifts by one fourth of the shift of eye orientation, so that the VOR follows a quarter-angle rule.[37]

The pulleys form a natural mechanical substrate for Listing's law and several other previously mysterious aspects of ocular kinematics.[15] Figure 9 is a side view of a diagrammatic globe showing a horizontal rectus EOM in the top panel. The rotational axis of the rectus EOM is perpendicular to the line connecting its pulley with the scleral insertion. Thus the rotational axis of the horizontal rectus EOM is vertical in straight-ahead gaze. Now consider the situation during visual fixation of a horizontally centered target at an angular elevation of angle α. If the distance from the pulley to the globe center D_1 is equal to the distance from the insertion to the globe center D_2, then the rotational axis tilts posteriorly by angle $\alpha/2$, precisely the requirement of Listing's law. A recent study of EOM path inflections in secondary gaze positions such as this example has demonstrated that in straight-ahead gaze the four rectus pulleys are indeed located in the positions required by the half-angle rule (Clark and Demer, unpublished data, 2000).

For a physiologic VOR, an orbit obeying the half-angle rule would require a neural controller performing a complicated tensor multiplicative comparison between eye orientation and angular velocity, and would have to do so using both sensory and motor coordinate system transformations.[39] A simpler explanation involves a posterior shift in pulley positions during the VOR (Fig. 9, lower). Selective orbital layer contraction could displace the pulley posteriorly so that $D_1 = 3D_2$. This would shift the rotational axis of the EOM by approximately one fourth the change in eye orientation, implementing the quarter-angle rule. Separate motor neuron pools, or differing synaptic input weighting in the same motor neuron pool, could implement larger relative pulley motion during the VOR than during other types of eye movement. Motor neurons projecting to the orbital layer may be expected to have higher gain during the VOR than neurons projecting to the global layer. This idea is consistent with observations that motor unit

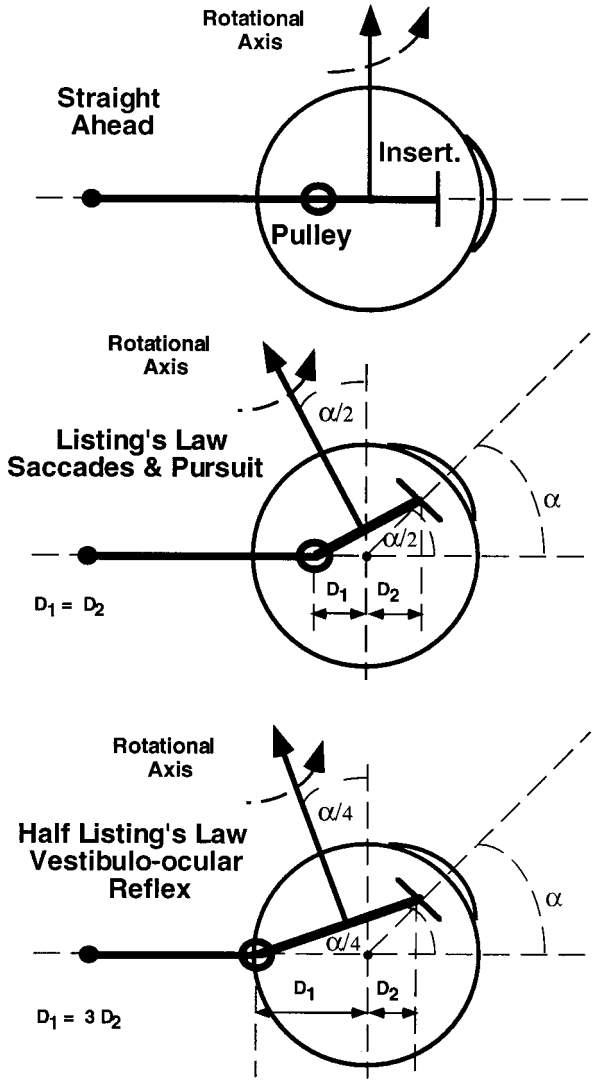

FIGURE 9. Effect of pulleys on the rotational axis of horizontal rectus EOMs. The orbit is viewed from a horizontal perspective. The rotational axis for any EOM is perpendicular to the line connecting the pulley to the scleral insertion and so is vertical in straight-ahead gaze (*top*). During saccades and pursuit eye movements with the eye in the secondary position of elevation of (small) angle α (*middle*), the distance D_1 from the pulley (*dark ring*) to the globe center is equal to distance D_2 from the insertion to the globe center. Thus, the rotational axis of the EOM tilts posteriorly by approximately angle $\alpha/2$. This satisfies the half-angle rule to implement Listing's law. The half-Listing's quarter-angle rule can be satisfied during the VOR (*lower*) if preferential contraction of global layer fibers posteriorly displace the pulley so that $D_1 = 3D_2$.

behavior may be specialized for particular types of eye movements.[40]

In tertiary (oblique) gaze positions, pulley behavior can still explain Listing's law as illustrated in Figure 10, a top view of a schematic orbit showing the MR and LR muscles. Beginning in primary position in the upper panel, the secondary positions of elevation and depression can be attained in conformity to Listing's half-angle rule as explained earlier, if the distance from the pulley to the globe center D_1 is equal to the distance from the insertion to the globe center D_2. Beginning in adduction as diagrammed in the lower panel, the tertiary positions of adducted elevation and adducted depression can be attained in conformity to Listing's law once again if the distance from the pulley to the globe center D_1 is equal to the distance from the insertion to the globe center D_2. Distances D_1 and D_2 are referenced to the globe, not to the orbit. To implement Listing's law, shifts in the anteroposterior position of the pulleys must occur when beginning in the secondary positions of abduction, elevation, or depression, and moving into tertiary positions. In cats, the most powerful and fatigue-resistant motor units of the LR muscle, comprising of 27% of all units, consist of single neurons innervating fibers in both the orbital and global layers.[19] These bilayer motor units would command similar contraction in the two layers, an arrangement convenient to maintain the position of the pulley relative to the EOM insertion in secondary gaze positions as required for the half-angle rule.

Indirect support for the functional role of the orbital layer in pulley repositioning is provided by the LPS muscle, the elevator of the eyelid. The LPS makes a path inflection from horizontal to nearly vertical near the location of the SR pulley and can therefore be considered to act through a pulley. However, that there is no kinematic necessity for precise

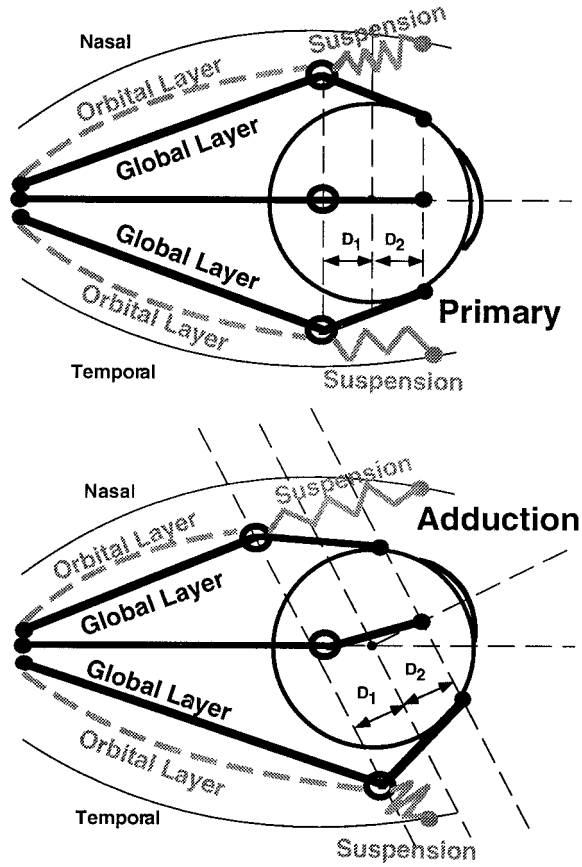

FIGURE 10. Superior view of diagrammatic orbit showing the shifts in horizontal rectus pulley position required to maintain the Listing's half-angle relationship in the tertiary positions of adducted elevation and adducted depression. Pulleys are depicted as *dark rings*. Paths of the global layers of each EOM are shown in *black*, whereas the orbital layers inserting in the pulleys twice are shown in *gray*. The suspension of the horizontal rectus pulleys, consisting of SM, collagen, and elastin, originates from the anterior orbital bones and is also shown in *gray*.

control of the LPS inflection point is consistent with the absence of an orbital layer in the LPS.

The plausibility of the postulated anteroposterior pulley shifts is supported by MRI images of EOM paths in Figure 1B. Note the similarity of the horizontal rectus paths to the diagram in Figure 10 and the appropriate direction of the shifts in pulley structures denoted with the arrowheads, suggesting that distances D_1 and D_2 may actually be roughly equal in living subjects. Note that the inflections observed in axial images of the horizontal rectus EOMs in the secondary positions of abduction and adduction may not exactly reflect the points of inflection out of the axial plane in tertiary gaze positions. A quantitative test of the hypothesis illustrated in Figure 10 would require precise measurements of rectus EOM paths in 3-D. However, the qualitative aspects of EOM path evident from these images are consistent with this hypothesis. The orbital layer insertion of each EOM on its corresponding pulley seems ideally suited to implement the necessary pulley repositioning against its elastic and SM suspensions that would, on relaxation of orbital layer fibers, move the pulley forward. For visually guided or volitional eye movements conforming to Listing's law around primary gaze, global layer fibers would be expected to receive motor commands at roughly the same gain as orbital layer fibers, to maintain the required relationship between the pulley and the scleral insertion.

It has been observed experimentally that Listing's planes for the two eyes rotate temporally during convergence, corresponding to the relative excyclotorsion in depression and incyclotorsion in elevation[41-43] necessary to maintain alignment of corresponding retinal meridians during near viewing. Thus, during the binocular viewing of near and far targets aligned on one eye, Listing's plane for that unmoving eye nevertheless tilts in association with the vergence movement of the other eye.[43] This tilting of Listing's plane has been interpreted as confirmation of the neural nature of Listing's law but could alternatively be attributed to a symmetrical reconfiguration of rectus pulleys during vergence as illustrated in Figure 11. Suitable reconfiguration of pulleys could include a nasal displacement of the vertical rectus pulleys due to contraction of the peribulbar SM and due to tension from posterior displacement of the MR pulley by its orbital layer transmitted to the vertical rectus pulleys through fibroelastic intercouplings. The resultant nasal displacement of the vertical rectus pulleys gives the vertical rectus EOMs an extorting action in depression and an intorting action in elevation (Fig. 11), corresponding to temporal tilting of Listing's plane in each eye. It has been proposed by van Rijn and van den Berg[41] that a form of Hering's law of equal innervation exists for the vergence system, such that both eyes receive symmetric version commands for remote targets, and mirror symmetric vergence commands for near targets. We extend this suggestion to propose that symmetric control may be applied to the pulleys through the orbital layer rectus fibers and peribulbar SM, so that pulleys in both orbits are configured with mirror symmetry during convergence, regardless of superimposed conjugate gaze. Such a configuration could explain the otherwise perplexing finding in monkeys of mirror units in the abducens[40,44] and oculomotor nuclei.[40] In these monkeys fixating near and far targets aligned with one eye, identified motoneurons specifically projecting to striated EOMs of the aligned (and nonmoving) eye apparently fired in response to the monocular position of the opposite eye.[42] This otherwise astonishing finding could be reconciled if the recorded motoneurons projected to the orbital layer of the aligned eye and were reconfiguring the pulleys of the involved EOMs as vergence changed.

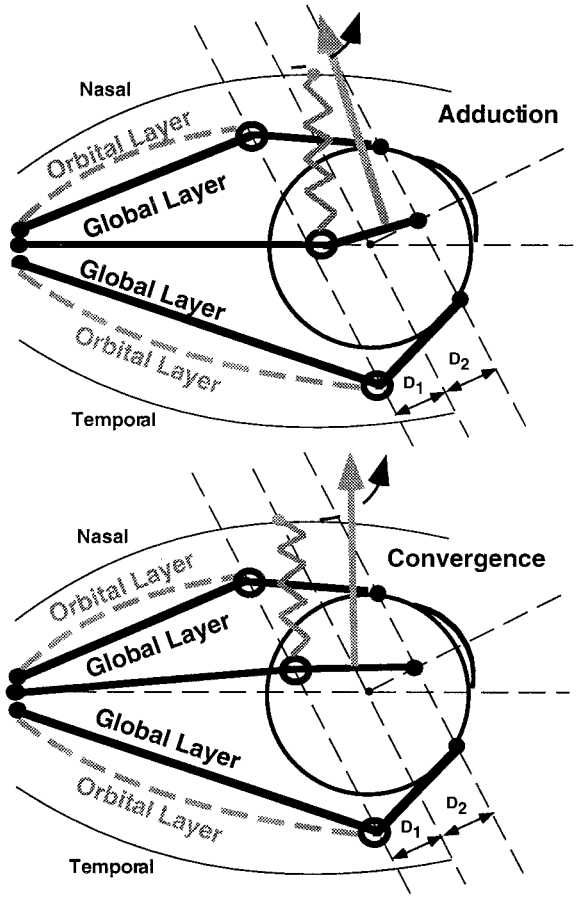

FIGURE 11. Superior view of diagrammatic representation of putative mechanical basis for temporal tilting of Listing's plane during convergence, perhaps implemented by nasal displacement of the vertical rectus pulleys. Pulleys are depicted as *dark rings*. The axis of rotation of the vertical rectus EOM is shown by *gray arrows* for conjugate adduction (*top*) and convergence (*bottom*). Note that the rotational axis of the vertical rectus EOM tilts temporally in convergence compared with conjugate adduction, when the vertical rectus pulley is displaced nasally. The peribulbar SM, known to have a morphology consistent with implementing this nasal displacement of the vertical rectus pulleys in convergence, is shown in *gray*.

None of the described arguments prohibits the brain from delivering commands to the EOMs to violate Listing's law.[15] As proposed, the pulley system may well be specifically configured to violate Listing's law during the VOR, and neural commands to the oblique EOMs, during the VOR or during sleep, could directly violate Listing's law as well. However, if no contrary neural command were given, eye movement commands could be specified in two dimensions, because single-unit recordings indicate they are in most premotor structures[35] and the pulley system would mechanically execute 3-D eye movements conforming to Listing's law.[15] The pulleys would render horizontal and vertical eye position commands essentially commutative in the mathematical sense, simplifying central neural control.[15,45] Any behavior of the oculomotor system that is noncommutative, such as maintenance of gaze stability

in darkness during various sequences of head rotations, would require explicit specification in the brain.[46]

Implications of the Active-Pulley Hypothesis for Ocular Dynamics

The active-pulley hypothesis has major implications for ocular dynamics. Raphan[45] and Quaia and Optican[15] have argued that by implementing a linear plant, pulleys would effectively permit motor commands to the global layer to consist of the rate of change of desired eye orientation and its simple mathematical integral. The pulley system would thus function as an analog computer to convert rate of change in desired eye orientation into the kinematically required 3-D eye velocity and would make eye position commands essentially commutative. This simplifies the otherwise complex problem of matching the pulse to the step of saccadic innervation.[15]

Electromyographic (EMG) recordings in the human LR global layer demonstrate both a phasic pulse and tonic step of activity during saccades, the former necessary to drive the formidable viscous load imposed by the relaxing antagonist EOM and the latter necessary to oppose the lesser elastic load as position is maintained.[47] Recordings of tension at the insertions of simian horizontal rectus EOMs confirm the presence of both saccadic pulses and steps.[48] In the human orbital layer, however, EMG shows only a step of activity during saccades, whereas the global layer exhibits both pulses and steps.[47] Orbital layer fibers have lower recruitment thresholds than global layer fibers,[20,47,49] prompting Collins[47] to propose that the orbital layer may have a special role in fixation. The insight that the orbital layer inserts on the pulley permits an alternative interpretation. The mechanical load on the orbital layer is likely to be dominated by elasticity of the attached pulley suspension. Collins has pointed out that the main load on an EOM attached to the globe is viscosity arising from the relaxing antagonist EOM. A phasic pulse of force in the orbital layer is unnecessary to achieve brisk pulley motion against a mainly elastic load. However, this elastic loading by passive connective tissue requires that orbital layer fibers maintain active tension throughout the oculomotor range to avoid slack. In contrast, global layer fibers remain under tension, even when relaxed, because of stretching by the antagonist EOM. The active-pulley hypothesis predicts that motor neurons preferentially innervating fibers in the orbital layer should, during saccades, exhibit step but not pulse changes in activity. Many such tonic motor neurons have been found in the abducens and oculomotor nuclei.[40]

Implications for Muscle Fiber Types

The active-pulley hypothesis may partially account for the complex variety of fiber types in EOMs, starting from the premise that fiber characteristics are adapted to their physiologic demands.[50] Approximately 80% of fibers in the orbital layer of each EOM are fast-twitch–generating SIFs resembling mammalian skeletal muscle fibers, whereas 20% are MIFs that either do not conduct action potentials or do so only in their central portions.[16] Orbital SIFs are specialized for intense oxidative metabolism and fatigue resistance.[16] The vascular supply in the orbital layer is high,[21] approximately 50% greater in humans than the well-perfused global layer.[51] The high metabolism, fatigue resistance, and luxurious blood supply of the numerous orbital SIFs are tailored to their continuous elastic loading by the pulley suspensions. The expression of unique myosin isoforms in orbital SIFs may also be related to the requirements of fast-twitch capability against continuous loading, because alterations in EOM activity patterns can change EOM-specific myosin heavy chain gene expression.[52] However, the function of the relatively sparse and primitive orbital MIFs remains unclear.

Approximately 90% of fibers in the global layer are fast-twitch–generating SIFs, whereas 10% are slow, non-twitch MIFs resembling those of amphibians.[16] The SIFs are often divided into three types—red, intermediate, and white—distinguished by their density of mitochondria and fatigue resistance.[16] The largest and most granular red SIFs, constituting approximately 33% of all global fibers, are very similar to orbital SIFs and are highly fatigue resistant, whereas the intermediate and white SIFs have progressively lower fatigue resistance.[16] The predominant static loading of the global layer by the moderate contractile force of antagonist EOM accounts for the global layer's higher overall recruitment threshold than the orbital layer and the lesser oxidative, vascular, and fatigue-resistant features of orbital SIFs. However, during saccades the high viscous loading of the global layer by the relaxing antagonist EOM requires the high transient force that intermediate and white SIFs are well suited to provide. The function of the small number of global MIFs remains obscure.

Implications for Strabismus

Orbital SIFs are the last EOM fiber type to mature to adult features and do so after birth during the establishment of binocular alignment.[17,53] Nemestrina monkeys, a macaque species with a high prevalence of naturally occurring strabismus, show evidence of a role of orbital layer abnormalities in the pathogenesis of strabismus. These monkeys transiently exhibit tubular aggregates only in orbital SIFs during the first 6 months of life, whereas fascicularis monkeys exhibit neither the tubular aggregates in the orbital layer nor naturally occurring strabismus.[17]

Treatment of strabismus probably affects the action of orbital EOM layers on their pulleys. Botulinum toxin treatment of strabismus produces its most lasting effects on orbital SIFs[21] and may therefore alter pulley behavior. Strabismus surgery that alters the relationships between EOM insertions and pulleys probably produces unintended effects that should be better understood and perhaps considered in surgical planning. In particular, any pulley manipulation compromising the orderly relationship between eye orientation and the rotational axes of EOMs would compromise neural control of eye movement[15] and would be expected to produce at least dynamic binocular misalignments in tertiary gaze positions. Noncommutativity of ocular rotations could also occur in patients who have strabismus with pulley abnormalities.

Acknowledgments

The authors thank Joel M. Miller and Douglas Tweed for helpful suggestions; James Lynch for generously providing an anatomic specimen; and Nicolasa De Salles, Frank Henriquez, and Zita Jian for technical assistance.

References

1. Miller JM, Robins D. Extraocular muscle sideslip and orbital geometry in monkeys. *Vision Res.* 1987;27:381–392.

2. Simonsz HJ, Harting F, de Waal BJ, Verbeeten BWJM. Sideways displacement and curved path of recti eye muscles. *Arch Ophthalmol.* 1985;103:124–128.
3. Miller JM. Functional anatomy of normal human rectus muscles. *Vision Res.* 1989;29:223–240.
4. Miller JM, Demer JL, Rosenbaum AL. Effect of transposition surgery on rectus muscle paths by magnetic resonance imaging. *Ophthalmology.* 1993;100:475–487.
5. Clark RA, Rosenbaum AL, Demer JL. Magnetic resonance imaging after surgical transposition defines the anteroposterior location of the rectus muscle pulleys. *J Am Assoc Pediatr Ophthalmol Strabismus.* 1999;3:9–14.
6. Demer JL, Miller JM, Poukens V, Vinters HV, Glasgow BJ. Evidence for fibromuscular pulleys of the recti extraocular muscles. *Invest Ophthalmol Vis Sci.* 1995;36:1125–1136.
7. Demer JL, Poukens V, Miller JM, Micevych P. Innervation of extraocular pulley smooth muscle in monkeys and humans. *Invest Ophthalmol Vis Sci.* 1997;38:1774–1785.
8. Koornneef L. *Spatial Aspects of Orbital Musculo-fibrous Tissue in Man.* Amsterdam: Swets & Zeitlinger; 1977.
9. Koornneef L. Orbital septa: anatomy and function. *Ophthalmology.* 1979;86:876–880.
10. Porter JD, Poukens V, Baker RS, Demer JL. Structure-function correlations in the human medial rectus extraocular muscle pulleys. *Invest Ophthalmol Vis Sci.* 1996;37:468–472.
11. Christiano AM, Uitto J. Molecular pathology of the elastic fibers. *J Invest Dermatol.* 1994;103:53S–57S.
12. Demer JL, Miller JM, Poukens V. Surgical implications of the rectus extraocular muscle pulleys. *J Pediatr Ophthalmol Strabismus.* 1996;33:208–218.
13. Clark RA, Miller JM, Demer JL. Location and stability of rectus muscle pulleys inferred from muscle paths. *Invest Ophthalmol Vis Sci.* 1997;38:227–240.
14. Clark RA, Miller JM, Rosenbaum AL, Demer JL. Heterotopic rectus muscle pulleys or oblique muscle dysfunction? *J Am Assoc Pediatr Ophthalmol Strabismus.* 1998;2:17–25.
15. Quaia C, Optican LM. Commutative saccadic generator is sufficient to control a 3-D ocular plant with pulleys. *J Neurophysiol.* 1998; 79:3197–3215.
16. Porter JD, Baker RS, Ragusa RJ, Brueckner JK. Extraocular muscles: Basic and clinical aspects of structure and function. *Surv Ophthalmol.* 1995;39:451–484.
17. Porter JD, Baker RS. Developmental adaptations in the extraocular muscles of Macaca nemestrina may reflect a predisposition to strabismus. *Strabismus.* 1993;1:173–180.
18. Mayr R, Sottwchall J, Gruber H, Neuhuber W. Internal structure of cat extraocular muscle. *Anat Embyol.* 1975;148:24–34.
19. Shall MS, Goldberg SJ. Lateral rectus EMG and contractile responses elicited by cat abducens motoneurons. *Muscle Nerve.* 1995;18:948–955.
20. Scott AB, Collins CC. Division of labor in human extraocular muscle. *Arch Ophthalmol.* 1973;90:319–322.
21. Spencer RF, Porter JD. Structural organization of the extraocular muscles. In: Buttner–Ennever J, ed. *Neuroanatomy of the Oculomotor System*. Amsterdam: Elsevier; 1988:33–79.
22. Demer JL, Miller JM. Orbital imaging in strabismus surgery. In: Rosenbaum AL, Santiago P, eds. *Advanced Strabismus Surgery: Principles and Surgical Techniques*. New York: Mosby; 1999:84–98.
23. Sheehan DC, Hrapchak BB. *Theory and Practice of Histotechnology*. St. Louis: Mosby; 1973:95–116.
24. Sternberger LA. *Immunocytochemistry.* 2nd ed. New York: Wiley, 1979.
25. Müller H. Uber einen glatten Muskel in der Augenhohle des Menschen and dur Saugethiere. *Z Wiss Zool.* 1858;9:541.
26. Page RE. The distribution and innervation of the extraocular smooth muscle in the orbit of the rat. *Acta Anat.* 1973;85:10–18.
27. Goldberg SJ, Wilson KE, Shall MS. Summation of extraocular motor unit tensions in the lateral rectus muscle of the cat. *Muscle Nerve.* 1997;20:1229–1235.
28. Goldberg SJ, Meredith MA, Shall MS. Extraocular motor unit and whole-muscle responses in the lateral rectus muscle of the squirrel monkey. *J Neurosci.* 1998;18:10629–10639.
29. Pachter B. Fiber composition of the superior rectus extraocular muscle of the rhesus macaque. *J. Morphol.* 1982;174:237–250.
30. Oh SY, Poukens V, Demer JL. Quantitative analysis of rectus extraocular muscle layers in monkey and human. *Abstracts of 26th Annual Meeting of the American Association for Pediatric Ophthalmology and Strabismus.* In press.
31. Haslwanter T. Mathematics of three-dimensional eye rotations. *Vision Res.* 1995;35:1727–1739.
32. Tweed D, Vilis T. Implications of rotational kinematics for the oculomotor system in three dimensions. *J Neurophysiol.* 1987;58: 832–849.
33. Tweed D, Vilis T. Geometric relations of eye position and velocity vectors during saccades. *Vision Res.* 1990;30:111–127.
34. van den Berg AV. Kinematics of eye movement control. *Proc R Soc Lond B Biol Sci.* 1995;260:191–197.
35. Hepp K. Oculomotor control: Listing's law and all that. *Cur Opin Neurobiol.* 1994;4:862–868.
36. van Opstal J, Hepp K, Suzuki Y, Henn V. Role of the monkey nucleus reticularis tegmenti pontis in the stabilization of Listing's plane. *J Neurosci.* 1996;16:7284–7296.
37. Misslisch H, Tweed D, Fetter M, Sievering D, Koenig E. Rotational kinematics of the human vestibuloocular reflex, III: Listing's law. *J Neurophysiol.* 1994;72:2490–2502.
38. Nakayama K, Balliet R. Listing's law, eye position sense, and perception of the vertical. *Vision Res.* 1977;17:453–457.
39. Smith MA, Crawford JD. Neural control of rotational kinematics within realistic vestibuloocular coordinate systems. *J Neurophysiol.* 1998;80:2295–2315.
40. Henn V, Cohen B. Eye muscle motor neurons with different functional characteristics. *Exp Brain Res.* 1972;45:561–568.
41. van Rijn LJ, van den Berg AV. Binocular eye orientation during fixations: Listing's law extended to include eye vergence. *Vision Res.* 1993;33:691–708.
42. Somani RAB, Desouze JFX, Tweed D, Vilis T. Visual test of Listing's law during vergence. *Vision Res.* 1998;38:911–923.
43. Stefen H, Walker MF, Zee DS. Rotation of Listing's plane with convergence: Independence from eye position. *Invest Ophthalmol Vis Sci.* 2000;41:715–721.
44. Zhou W, King WM. Premotor commands encode monocular eye movements. *Nature.* 1998;393:692–695.
45. Raphan T. Modeling control of eye orientation in three dimensions, I: role of muscle pulleys in determining saccadic trajectory. *J Neurophysiol.* 1998;79:2653–2667.
46. Tweed DB, Haslwanter TP, Happe V, Fetter M. Non-commutativity in the brain. *Nature.* 1999;399:261–263.
47. Collins CC. The human oculomotor control system. In: Lennerstrand G, Bach-y-Rita P, ed. *Basic Mechanisms of Ocular Motility and Their Clinical Implications*. New York: Pergamon; 1975:145–180.
48. Miller JM, Robins D. Extraocular muscle forces in alert monkey. *Vision Res.* 1992;32:1099–1113.
49. Barmack NH. Laminar organization of the extraocular muscles of the rabbit. *Exp Neurobiol.* 1978;59:304–321.
50. Porter JD, Hauser KF. Diversity and developmental regulation of extraocular muscle: progress and prospects. *Acta Anat.* 1993;147:197–206.
51. Oh S, Poukens V, Demer JL. Quantitative analysis of vascularity in human rectus extraocular muscle layers. [ARVO Abstract]. *Invest Ophthalmol Vis Sci.* In press.
52. Brueckner JK, Ashby LP, Prichard JR, Porter JD. Vestibulo-ocular pathways modulate extraocular muscle myosin expression patterns. *Cell Tissue Res.* 1999;295:477–484.
53. Spencer RF, McNeer KW. Morphology of the extraocular muscles in relation to the clinical manifestation of strabismus. In: Lennerstrand G, von Noorden GK, Campos EC, ed. *Strabismus and Amblyopia*. New York: Plenum Press; 1988:37–46.